A Review of Microsegregation Induced Banding Phenomena in Steels

John D. Verhoeven

(Submitted 11 November 1999; in revised form 22 February 2000)

A review is presented of banding in hypoeutectoid and hypereutectoid steels. The data available on hypereutectoid steels are quite limited and therefore a study is presented on banding in a 52100 steel. Similarities and differences are identified in the banding that occurs in commercial hypoeutectoid versus hypereutectoid steels. The distinct surface patterns of Damascus steels, which are nearly pure hypereutectoid steels, have recently been shown to be due to carbide banding. It is shown that the carbide banding in the 52100 steel occurs by a distinctly different mechanism than the carbide banding of the Damascus composition steels.

Keywords hypereutectic steels, hypereutectoid steels, microsegregation (banding)

1. Introduction

The dendritic nature of the solidification process in steels leads to microsegregation of impurities and alloying elements in the steel. One of the major consequences of this microsegregation is the formation of banded structures in wrought steel products. Such banding phenomena have been widely studied in hypoeutectoid steels and sparsely studied in hypereutectoid steels. This paper presents an extensive review of the literature on both types of steels along with some new data, mainly on hypereutectoid steels.

2. Experimental

Experiments were carried out on the four hypoeutectoid and two hypereutectoid steels listed in Table 1. All of the commercial steels were received in the form of 2.54 cm rounds, except the 15B21, which was in the form of 6 mm thick plate. Samples were cut from the round bars as 6 to 8 mm thick disks, which were sectioned into two pieces along a diameter. Similar sized pieces were cut from the plate. Individual samples were wired to a 3 mm diameter stainless steel sheathed type K thermocouple and inserted into a vertical resistance heated tube furnace under vacuum. The tube was back filled with Ar and after austenitization the samples were cooled at a range of cooling rates. The slowest cooling rates (≈10 °C/h) were obtained with a programmed controller and the fastest rates by forced air cooling ($\approx 7.4 \times 10^{-4}$ °C/h). Most samples were furnace cooled (≈400 °C/h) and faster intermediate rates were achieved by raising samples into the cooler part of the furnace. All of the reported cooling rates were taken at the arrest temperature for the eutectoid reaction with the thermocouple embedded in a hole drilled in the sample. Data were collected as computer files and the reported arrest temperatures taken as the temperature where the first derivative of the time/temperature plots abruptly changed slope. All metallographic samples were prepared on sectioned surfaces to avoid possible surface contamination effects.

John D. Verhoeven, Department of Materials Science and Engineering, Iowa State University, Ames, IA 50011.

3. Hypoeutectoid Steels

The most common form of banded microstructures is the ferrite/pearlite (f/p) banding, which occurs widely in plain carbon steels and in slow cooled low alloy AISI steels. In such structures, longitudinal micrographs display alternating bands of ferrite and pearlite lined up in the direction of the deformation used to form the wrought steel product. To demonstrate the ubiquity of this microstructure in hypoeutectoid steels, the four hypoeutectoid steels of Table 1 were studied. All four steels showed modest amounts of f/p banding in the as-received state. However, after austenitization at temperatures of 870 to 935 °C followed by furnace cooling, all four steels displayed strong f/p banding on longitudinal sections, as illustrated in Fig. 1.

As might be expected for such a ubiquitous microstructure, there exists a large literature on this structure extending back to the beginning of the twentieth century. Some of the first investigators[1–6] discovered special etchants to reveal microsegregation and the etchants are now named after them, *e.g.*, Stead's and Oberhoffer's etches. Early recognition of the ubiquity of the banded structure is illustrated by Carpenter and Robertson's[7] classification of the banded ferrite morphology along with the Widmanstätten ferrite morphology as "normal ferrite structures." The now widely used term of "banding" was slow in acceptance. Early studies, in addition to using the term banding, often referred to these structures as ferrite lines[6,7] or ghost lines,[8–12] particularly if the bandwidth was large. The transition to exclusive use of the term "banding" appears to have occurred in the decade of the 1930s or shortly after.

It is now clear that these banded microstructures arise because of microsegregation of some alloying element, X, in the hypoeutectoid Fe-C-X steel. This microsegregation is produced by the dendritic growth mode of steel during solidification. Dendritic solidification virtually always causes the X element to concentrate in the interdendritic regions (IRs) and leaves the X

Table 1 Chemical analysis of steels examined in this study (all compositions in this paper are in weight percent)

Steel	C	Mn	P	S	Si	Ni	Cr	Mo	Cu
15B21	0.20	1.01	0.013	0.004	0.20	•	•	•	•
1018	0.17	0.70	0.007	0.020	0.20	0.02	0.04	<0.01	0.01
1045	0.43	0.77	0.011	0.039	0.23	0.07	0.13	<0.01	0.22
1144	0.43	1.50	0.017	0.228	0.21	<0.01	0.03	<0.01	0.01
52100	1.03	0.30	0.19	0.014	0.23	0.06	1.28	<0.01	0.10
Damascus	1.41	<0.01	0.098	0.006	0.05	0.04	<0.01	<0.01	0.09

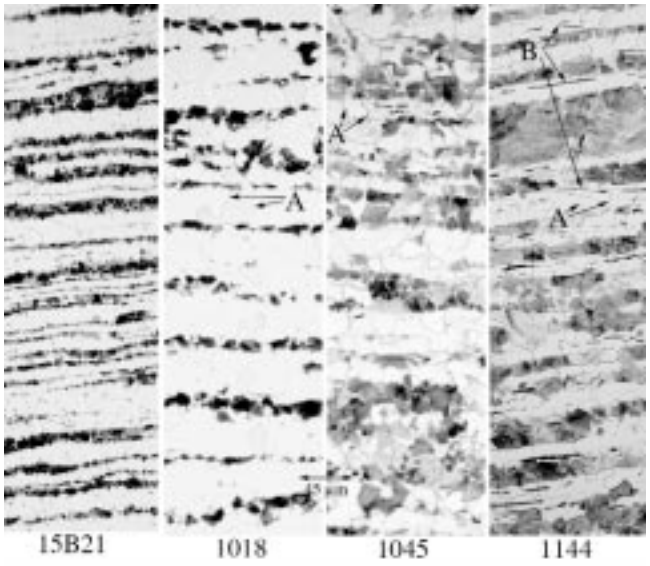

Fig. 1 Banded microstructure of four steels after austenitization and furnace cooling

concentration lower in the dendritic regions (DRs), and the concentration difference will be called dendritic microsegregation. In a wrought alloy, the DRs, as well as the IRs, will have been strung out into stringers parallel to the dominant flow directions of the mechanical deformation. Because microsegregation is the root cause of banding, it is the microsegregated elements that cause the ferrite and pearlite to form preferentially along the stringers. Apparently, the first suggestion that such microsegregation was the cause of banding was made by Stead.[1,2] His Cu based etchants, *i.e.*, Stead's etches, are extremely effective at revealing the relative P concentration in steels. At the low P level present in steels, they are more sensitive than modern electron probe microanalysis (EPMA) techniques at revealing the presence of microsegregation. Stead's etches cause high P regions to appear white relative to lower P regions, and interestingly, this contrast occurs independently of the ferrite/pearlite microstructure present in the background of a micrograph. Based on his early studies, Stead concluded that there was a one-to-one correspondence between ferrite bands and high P bands and that the banding was therefore produced by microsegregation of P. Later studies[10] questioned the requirement of P for producing a banded structure, and there is good evidence[13] that although P may cause banding in laboratory steels, it is unlikely that it plays a significant role in commercial steels. The large body of research on banded steels now offers overwhelming evidence that the phenomenon is a result of microsegregation of one or more X elements in Fe-C-X alloys.

Prior to discussing the specific characteristics of banding in hypoeutectoid steels, a short discussion will be presented on our present understanding of the relationship between the microsegregation produced by dendritic growth in the ingot and the microsegregation observed between the alternating bands in a f/p banded steel.

4. Mechanism of p/f Banding

The diffusion coefficients, D_X, of the various alloying elements, X, in steels are very much smaller than the value of the diffusion coefficient of C in steel, D_C. This interesting fact plays a strong role in the possible mechanisms for formation of the banded f/p structure in steel. It is clear that in the banded microstructure there exists a very large change in C concentration between bands, as it must go from a value of around 0.02% in a ferrite band to a value of around 0.77% in the pearlite band. There are two possible origins of this microsegregation, which, adopting terminology from Kirkaldy *et al.*,[13] may be termed presegregation and transegregation. Presegregation refers to the microsegregation that has occurred in the dendritic solidification process plus any reduction in the amplitude of this dendritic microsegregation during the cooldown to the start of ferrite precipitation, *i.e.*, to the A_{r3} temperature. Transegregation refers to any segregation that occurs during the solid state transformation from austenite to ferrite + pearlite.

Consider first the solidification of a pure Fe-C alloy. Both experimental and theoretical arguments[14] have shown that due to the high value of D_C in austenite, coupled with the small distance between dendrite arms, virtually all of the dendritic microsegregation of C between austenite dendrite arms is homogenized during solidification or very shortly after the final interdendritic liquid has solidified. This means that the presegregation of C is essentially zero in a pure Fe-C alloy. Consequently, one would not expect banding to be able to occur in high purity Fe-C alloys, as the austenite is homogeneous at the temperature where ferrite nucleates, A_{r3}, *i.e*, there is no microsegregation remaining.

Consider now the solidification of an Fe-C-X alloy. After this alloy has cooled to the A_{r3} temperature, the dendritic microsegregation of X will remain in the austenite because of the low value of D_X in austenite. This presegregation of X will, in turn, produce a presegregation of C due to the fact that X has an effect on the C activity. The high value of D_C means that the C concentration will adjust to constant C activity, which, in the presence of the X presegregation, means their will also be a C presegregation. Such a

condition has been termed a transient equilibrium by Kirkaldy and Purdy[15] and Brown and Kirkaldy,[16] and they have done experiments with common alloying elements in steel that allows one to calculate how much a given presegregation of the X element in austenite, $\Delta C_X(\gamma)$, will change the C concentration in austenite, $\Delta C_C(\gamma)$. Suppose, for example, that in a Fe-0.3C-1.0Mn alloy the presegregation of the Mn runs from a minimum of 0.5% to a maximum of 1.5%. Their data[15,16] show that this $\Delta C_{Mn}(\gamma)$ of 1% will produce a corresponding C microsegregation of $\Delta C_C(\gamma)$ = 0.03%, *i.e.*, the C concentration will vary from 0.27 to 0.33%, in the austenite. This $\Delta C_C(\gamma)$ leads to two effects upon adjacent presegregated band regions: (1) the difference in carbon composition, and (2) a difference in the A_{r3} temperature. The first effect will be negligible in the final banded structure because the change in C composition in ferrite inherited from the $\Delta C_C(\gamma)$ is reduced by the factor of the partition coefficient, *k*, of C between austenite and ferrite, *i.e.*, $\Delta C_C(\alpha) = k\Delta C_C(\gamma)$, where *k* = the ratio of the fraction C in ferrite to that in austenite at a given temperature, as determined by the phase diagram. For the Fe-C diagram, *k* varies from around 0.02 to 0.06. Hence, the 0.03% C for $\Delta C_C(\gamma)$ in the above example will produce a $\Delta C_C(\alpha)$ in the range of 0.0006 to 0.002% C in the ferrite formed, showing that the first effect will be essentially negligible.

However, the second effect of the presegregation of the Mn is not negligible. The reduction in A_{r3} at the high Mn regions (the IR bands) versus the low Mn regions (the DR bands) sets up the mechanism of transegregation. The ferrite will nucleate first along the locus of the bands with the higher A_{r3} temperature (the DR bands for X = Mn), and this will produce the bands of ferrite lying parallel to the deformation flow. Kirkaldy *et al.* have considered how the C presegregation will influence banding by showing how it affects the A_{e3} temperature. At the slower cooling rates where banding occurs, they assume that the A_{e3} provides a good approximation of A_{r3}. All the alloying elements segregate to the IRs and this, in turn, causes C to segregate either to the IRs or the DRs depending on whether the alloying element raises or lowers the C activity. Then, by considering the corresponding effect of C on the Fe-C-X phase diagram, they determine the qualitative effect on A_{e3}. Their results show that all of the common alloying elements except Ni tend to increase the difference in A_{e3} between IR and DR bands and therefore tend to enhance the tendency for banding due to the transegregation mechanism.

The transegregation mechanism operates as follows. The ferrite nucleates first along the sets of either the DR bands or the IR bands, depending on which set has the higher A_{r3} temperature. So long as the ferrite/austenite growth front moves into the austenite along a planar or nearly planar geometry, it pushes the C ejected from the nearly pure ferritic iron ahead of the advancing interface plane into the austenite. Hence, if the ferrite nucleates along the DR bands, and grows with near planar fronts toward the IR bands, it will concentrate C in the IR bands and pearlite will finally form there. There is little doubt that this is the mechanism of C mass transport that occurs in f/p band formation, because the ferrite is often observed[4,12,17,18] to have a bamboo structure with the ferrite/ferrite grain boundaries revealing that the ferrite growth direction was at right angles to the band direction, *i.e.*, from DR bands to IR bands or *vice versa*. Such boundaries are shown at the arrows marked A in Fig. 1.

Early in the century, it was recognized that to better explain banding, new experimental techniques would be required to adequately characterize the chemical microsegregation present in banded steels,[19] and such techniques were developed around midcentury. Initially, the new techniques used to study banded steels were microradiography[20,21] and autoradiography.[22] Later the more quantitative method of EPMA was utilized starting, apparently, with the work of Philibert and Bizouard[23] and followed by numerous studies.[11,12,18,24–28]

5. Characteristics of Banding in Hypoeutectoid Steels

The f/p banding phenomenon arises from a change in composition between the DR and IR bands. This change in composition can give rise to a variety of banded microstructures in steels. The varieties may be partitioned into two types: structural banding and chemical banding. In structural banding, the microconstituents vary between alternate bands. The p/f banding is an example of structural banding and it is the type of banding seen most often in plain carbon steels. In alloy steels, the following additional types of structural banding often occur, depending on cooling rates: f/b, f/m, p/b, p/m, b/m,[11,24,29–32] where b and m refer to bainite and martensite, respectively. Whereas structural banding is produced by changes in the A_{r3} temperature between the DR and IR bands, chemical banding results from an etching effect. Special etches are able to etch regions of high X element concentration darker or lighter than the regions of lower concentration. Hence, bands appear in structures that are 100% martensite[12,30,33] or in structures that are 100% bainite.[32] In addition, if the microsegregated X element is P, the use of Stead's etch may show light/dark bands in a two-phase f/p matrix, where the bands do not correspond specifically to either the pearlite or ferrite microconstituent.

The important characteristics of f/p banding may be listed as follows.

1. It has been known since the earliest studies[8,34] that the banded microstructure appears after a single cooldown from the austenite region, but only if the cooling rates are relatively slow. This result is illustrated nicely by Samuals,[12] who presents a series of micrographs for samples cooled at increasing rates showing that the banding disappears at rates of 1500 to 3000 °C/h in a 1.75% Mn/0.25% C steel. However, if the nonbanded fast cooled steel is reaustenitized and cooled at 300 °C/h, the bands return. The importance of cooling rate has been established by many investigations.[2,5,8,12,17,18,35–40] The critical cooling rate required to eliminate f/p bands is a function of the steel and its processing history. A few studies have determined the critical cooling rates required to eliminate p/f banding.[12,18,38,40] The values appear to have a fairly large range, from around 1200 °C/h[12] to around 1.8×10^4 °C/h.[40] Such variability was qualitatively confirmed in this work. The four steels of Fig. 1 were cooled in stagnant air and forced air, which produced cooling rates of $\approx 2.7 \times 10^4$ and $\approx 7.5 \times 10^{-4}$ °C/h, respectively. The stagnant air cooling rate eliminated the banding in only the 1045 steel. The forced air

cooling rate completely eliminated banding in the 15B21 and 1018 steels, but a few isolated bands remained in the 1144 steel, and these were found to coincide with those sulfide stringer bands containing the smaller sized sulfides present in this steel.

2. If the amplitude of the microsegregation is reduced by diffusion during a high-temperature heat treatment, the p/f banding can be permanently eliminated.[2,7,10,12,17,20,29,30,37,41–43] The amount of the reduction required to eliminate p/f banding has been shown to be less than that required to eliminate banding in tempered martensite structures. In a clever set of isothermal transformation experiments, Jatzak *et al.*[30] demonstrated that the level of microsegregation remaining in a 4340 steel after a 6 h 1200 °C anneal is no longer adequate to produce f/p bands, but it is adequate to produce m/p bands in steels quenched after partial transformation. In fact, even a 200 h anneal at 1200 °C was not adequate to completely eliminate the m/p bands. In addition, studies have shown that in some steels[33,44] a hold of only 10 min at 1320 °C will eliminate p/f banding, but the banding is not permanently eliminated as it can be made to return on subsequent deformation. It seems likely that some subtle effect worthy of additional research is operating here, because if diffusion during this thermal treatment were adequate to drop the microsegregation amplitude enough to eliminate banding in the as-rolled steel, subsequent rolling would not allow it to return. (Perhaps the 1320 °C anneal is adding grain boundary pinning sites so that the return of the banding is due to a reduced austenite grain size after the subsequent rolling and reaustenitization that was employed.)
3. The ferrite band spacing determined metallographically, S_f, may be compared to the microchemical band spacing determined with EPMA, S_m. Most studies[12,18,24,26] find a 1:1 correspondence between these two spacings. However, as discussed in the following point, there appears to be some exceptions to this rule.
4. The f/p band formation may be eliminated by growing the austenite grains significantly larger than S_m because the ferrite bands nucleate on prior austenite grain boundaries along the microchemical bands.[7,12,18,24,26,36,43,45,46] In the absence of significant amounts of microsegregated second-phase particles, such as (Mn,Fe)S, the ferrite will only nucleate in the microchemical bands at locations where austenite grain boundaries cross them. To form a ferrite band geometry, the individual ferrite grains must nucleate close enough together along the microchemical band that they will connect together along the band centerline after only a small amount of growth. Experiments show that the banding disappears when the grain size is greater than S_m by factors of 2 to 3.[12,18,26] Grossterlinden *et al.*[18] also show that when the austenite grain size approaches the value required to eliminate banding, the ferrite band spacing, S_f, rises and exceeds S_m. This effect is attributed to an inadequate supply of austenite grain boundaries to nucleate ferrite bands in each microchemical band. This effect of increase in S_f at higher austenitizing temperatures has also been found by others.[35,47] In addition, Grossterlinden *et al.*[18] show that sometimes the ferrite spacing is reduced by a factor of 2, *i.e.*, $S_f = S_m/2$, due to formation of a double pearlite band. Apparently, in a rather homogeneous array of uniformly spaced ferrite bands, some ferrite bands halve their spacing by containing two pearlite bands. During band formation, two ferrite growth fronts approach the interferrite centerline from either side trapping an austenite layer between them. Carbon is ejected from each growth front into this austenite region, with the maximum %C obtained in the austenite at the two growth fronts. Their model assumes that in the $S_f = S_m/2$ case, the pearlite reaction is initiated on both of these growth fronts, but the pearlite so formed is not able to grow clear to the ferrite centerline.
5. Work by Grange[33] presents micrographs that allow estimates of both the primary and secondary dendrite spacings in the ingots. Comparing the f/p band spacing to these values, and accounting for the expected reduction in spacing due to mechanical deformation, it is found that the f/p band spacing corresponds to the primary dendrite arm spacing of the ingots rather than the secondary arm spacing.
6. Depending on the X element of the Fe-C-X alloy, the ferrite bands correspond to either the IRs or the DRs of the ingot. Following the suggestion of Pokorny and Pokorny,[24] elements causing the ferrite to lie in the IR bands will be called inverse banding elements, as opposed to direct banding elements, which cause the ferrite bands to form in the DR bands. (The term inverse was coined because ferrite in the IRs produces a C microsegregation inverted from that expected for nonequilibrium freezing of an FeC alloy.) Whether a given alloying element is a direct or inverse banding element depends on what it does to A_{r3} at the high compositions of the IR bands versus the lower compositions of the DR bands (Fig. 2). Elements that raise A_{r3} can be inverse banders at lower cooling rates or direct banders at higher cooling rates. However, elements that lower A_{r3} should always be direct banders. For air cooled steels, elements generally found to be direct banders (ferrite in the DR bands) are Mn, Ni, and Cr,

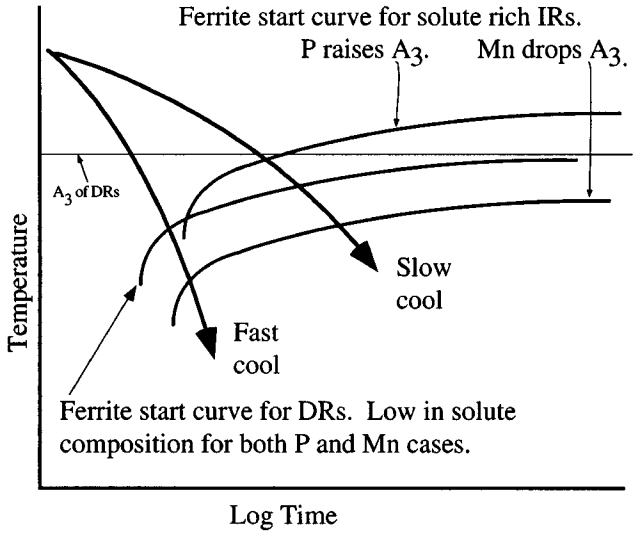

Fig. 2 Ferrite start curves on a continuous cooling transformation diagram

and those found to be inverse banders (ferrite in the IR bands) are P, Si, and Mo.[24] Note: laboratory experiments using isothermal transformation[30,48] can lead to different results, as the A_{r3} is now controlled by the IT diagram.

7. The morphology of the ferrite and pearlite bands depends on the type of deformation employed. It has been found that deformation to rod shapes produces cylindrical morphologies, while deformation to plate (sheet) shapes produces planar morphologies.[4,12,26,33,49] The planar morphologies in rolled sheet show considerable variability, however, with the extent of the bands in the longitudinal direction sometimes being greater than in the transverse direction.
8. The element Mn is a special case because it can cause either normal banding or inverse banding depending on the S level of the steel, as discussed below.
9. There have been several studies of the effect of banding on mechanical properties.[18,29,33,39,42,44,50] Generally, little to no effect is found on the anisotropy of tensile properties, but a significant anisotropy of reduction in area and impact properties is found. Banded steels invariably contain some degree of elongated inclusions, usually sulfides, in the IR bands, which can contribute to a reduction of transverse impact properties. Therefore, it is important to consider whether the anisotropy of area reduction and impact properties is due to the banding or to the elongated inclusions, and this is difficult to determine because treatments that remove banding often lead to spheroidization of elongated sulfides. Only some of the studies cited consider this problem.[29,33,44] The most careful of these studies[44] found that the reduction in anisotropy of mechanical properties after removal of p/f banding was due solely to the coarsening of the elongated sulfides by the treatment used to remove the banding.

In spite of the large literature on f/p banding, there remain some interesting questions concerning the mechanism of the banding formation. Three such questions will be considered.

5.1 Rate Dependence of F/P Banding

Grossterlinden *et al.*[18] attributed the loss of banding at high cooling rates to a reduction of the distance the austenite/ferrite interface can move to values less than the $S_m/2$ distance required to produce the C transport between ferrite and pearlite bands. They developed a finite difference analysis to predict the distance a planar austenite/ferrite interface can move versus cooling rate, and successfully predicted the critical cooling rates for the three steels studied. Their theory will be termed the "GKLP" theory. The experimental data of Samuals[12] suggests an alternate theory. In a steel of composition 0.25C, 1.75Mn, 0.34Si, and 0.24Cr, the micrographs show that the unbanded microstructure produced by high cooling rates contains ferrite exclusively in the Widmanstätten form. Hence, it is possible that the loss of the banding at high cooling rates could be due to a change in the ferrite precipitate morphology from the blocky grain boundary allotriomorphs (GBA) to the acicular shaped Widmanstätten morphology. The blocky ferrite morphology of GBAs is ideally suited to form the connected flat growth front along a ferrite band that is required to partition the C between alternate bands and thereby form pearlite between them. Carbon is transported in the direction of growth of the GBA precipitates. However, with the acicular ferrite that forms at high cooling rates, C atoms are transported at right angles to the fast growth direction of the ferrite plates or needles. Hence, as the acicular ferrite grows out from the centerlines of the microchemical bands, it does not transport the ejected C atoms in the proper direction to trap them between the bands. Consequently, the pearlite (or perhaps bainite or martensite at higher cooling rates) does not form as a band, but rather as a matrix between acicular ferrite.

The morphologies of the four steels of Fig. 1, cooled at rates sufficient to remove banding, were examined to test this alternate theory. Widmanstätten ferrite did not occur in the 1018 steel. It consisted of fine equiaxed ferrite grains of around 9 ≈m diameter interspersed with a small fraction of finer pearlite grains. Assuming $S_m = S_f$ for the furnace cooled samples, the ferrite diameters are $< S_m/2$, which is consistent with the GKLP theory. Both the 1045 and the 1144 steels displayed a thin GBA ferrite structure on pearlitic grains with a very minor amount of Widmanstätten sideplates. The thickness of the GBA averaged around 3 ≈m, which is again less than $S_m/2$, so that the results for these two steels are also consistent with the GKLP theory. The 15B21 steel contained two distinct microstructures, apparently due to a centerline segregation. It contained a mixture of Widmanstätten ferrite and bainite, with the ratio varying from roughly 70/30 in the center to 30/70 outside the center, respectively. In both cases, there was no evidence of banding, so for this steel, the loss of banding at high rates could be explained by the change of the ferrite morphology to the acicular Widmanstätten morphology.

5.2 Banding Caused by S

The element S is present in steel as compounds of FeS and/or (Mn,Fe)S with the relative amounts depending on the Mn level. These compounds form in the last liquid to freeze[21] and serve as markers to locate the IR bands of a banded steel. Some early literature[51,52,53] attributed the banding in steel to nucleation on these sulfide compounds. Later studies,[11,30,35,37,43] recognizing that ferrite bands sometimes form at the sulfide inclusions and sometimes do not, have concluded that the sulfide compounds do not control band formation. There is an interesting and subtle effect produced by the (Mn,Fe)S particles lying in the IR bands of a wrought steel that was pointed out by Kirkaldy *et al.*[54] They presented a thermodynamic analysis, which predicts that as the temperature drops, the Mn content of the solid (Mn, Fe)S that has formed in the IRs should increase, and this will, in turn, deplete the surrounding IR austenite of Mn. Their EPMA data show large Mn depletion in the ferrite surrounding large sulfides in skelp. These sulfide particles originated, not from dendritic segregation, but apparently from large sulfide segregates present in ingots, such as the well-known A segregate.[24]

Kiessling[55] presents data on two experimental studies that have documented the pickup of Mn by (Mn,Fe)S in annealed ingots versus as-cast ingots, as well as the Mn depletion zones around the (Mn,Fe)S particles. Clearly, the formation of low Mn austenite around (Mn,Fe)S particles by solid state diffusional processes during hot forging or rolling would favor formation of ferrite in the IR bands where these inclusions lie, as opposed to

having the ferrite lie in the DR bands as is normally found for low S steels. Two studies have shown[27,38] that the ferrite phase of f/p bands can be switched from DR bands to IR bands by increasing S levels. It seems likely that such strong conclusions as, "inclusions have very little or no influence on the formation of banded structures,"[11] might not be applicable to high S steels. Evidence that this is the case is presented in Fig. 1, which shows bands in the resulfurized steel, 1144, where it is consistently found that the ferrite bands surround the sulfides (arrows B). In addition, the banding in this 1144 steel persisted to higher cooling rates than found for the other three steels studied here, and the persistent bands were found along bands of sulfides. The resulfurized steels (11xx) contain relatively high levels of both S and Mn; they show copious (Mn,Fe)S particles in them and present a class of steels where it is likely that the band structure is controlled by the inclusions.

5.3 Banded Alignment

When observing strongly banded structures, it is amazing how well the bands line up with the deformation plane in sheet materials. As shown in the oldest study of the band morphology in sheet materials,[4] the band alignment on transverse and longitudial sections is often indistinguishable in strongly banded steels. An interesting question that has not been studied in the literature is how the dendritically produced segregation arrays become so well lined up into the two-dimensional planar bands during rolling or forging of sheet materials.

The discussion of band alignment will be presented for the case of inverse banding such as occurs with P or with (Mn,Fe)S banding. In this case, the ferrite bands will occur at the location of the IR array, which is produced by a combination of the dendritic solidification and the subsequent deformation. The geometry of the IR array produced by solidification may be described with the aid of Fig. 3 and 4. Figure 3 illustrates two possible arrays of dendrites from a view normal to the growth front. One might expect the hexagonal array to be the normal mode of growth because of its close packed nature, but there does not seem to be any strong theoretical reason for this to be true and our experiments on steel ingots, as well as directional solidification experiments on steel,[56] find both types of arrays. The left of Fig. 4 presents a three-dimensional sketch of a square array of four primary dendrites growing vertically. The secondary arms project orthogonally from the primaries, as required by the <100> growth directions for both primary and secondary arms of the cubic iron dendrites; and the spacing of the primary and secondary arms are given as λ_p and λ_s, respectively. The dark circles pinpoint the locations of the final liquid to freeze. The top center of Fig. 4 shows the dendrites growing perpendicular to the page, while the right picture shows a three-dimensional construction formed by connecting the final points of liquid to freeze. It can be seen that these points are arranged as a tetragonal lattice having a *c*-axis length of λ_s and an *a*-axis length of λ_p. This lattice will be called the IR lattice. Since each austenite grain forms with a particular orientation of dendrites, each grain will possess its own IR lattice. The maximum microsegregation in each grain will be located along the IR lattice of each grain, and the sulfide particles present in virtually all steels will also be located along this lattice.

For the hexagonal case of Fig. 3, the IR lattice is very similar to the square array, having the same *c/a* ratio, but with the hexagonal arrangement of points in the basal plane. In both cases, one ends up with a lattice of final points to freeze bearing a specific relation to the primary dendrite array that formed when the liquid solidified. The presence of the planar bands in the deformed ingots indicates that during deformation some set of IR lattice planes probably becomes aligned in the deformation plane during the hot deformation. If this suggestion is correct, it seems likely that it is one of the high density planes of the IR lattice, {100} or {110}, that lines up in the rolling plane, perhaps by some type of lattice rotation.

6. Hypereutectoid Steels

Banding is also a common microstructure observed in hypereutectoid steels where bands of carbides appear in a matrix that can be ferrite, pearlite, bainite, or martensite depending on the thermal history following the deformation process. There is a very sparce literature on hypereutectoid banding and there appears to be only one careful study of carbide banding in conventional steels.[39] Recent studies have shown[57,58] that carbide banding is responsible for the surface patterns on the famous Damascus blades of antiquity and that this banding requires repeated thermal cycling. Hence, there are two distinct thermal processes for producing carbide banding in hypereutectoid steels and these will be considered separately.

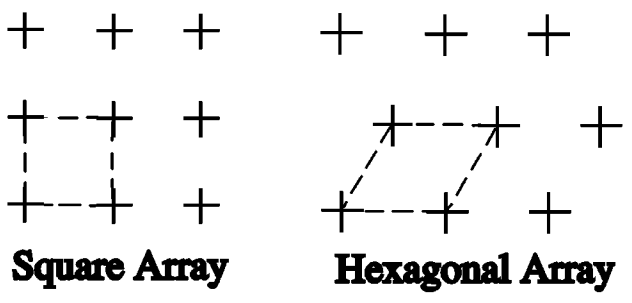

Fig. 3 Two possible geometric distributions of austenite dendrites growing toward you

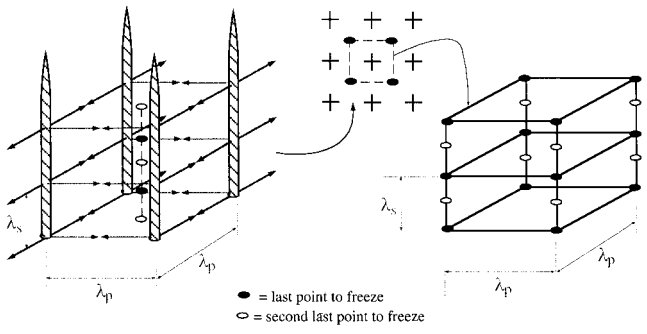

Fig. 4 Three-dimensional view of a square array of primary dendrites defining the IR lattice

6.1 Carbide Banding with Conventional Heat Treatments

There are two possible sources of carbides in these steels, primary carbides, which form directly from the liquid in the IRs, and secondary carbides, which form by solid state reactions. Primary carbides will result if the IR liquid reaches a carbide eutectic composition of the alloy, and this commonly occurs in hypereutectoid high alloy steels, such as many tool steels. In this case, carbide banding is inevitable in the wrought product as the carbides often cannot be made to dissolve into the austenite on forging and will simply remain in the steel and align during the hot working process. In low alloy hypoeutectoid steels, such as the common bearing steel 52100, primary carbides generally dissolve into the austenite during hot working, and banding may result from secondary carbide formation. One would expect that secondary carbide formation might lead to carbide banding similar to the ferrite banding for hypoeutectoid steels and this possibility is examined in the following discussions.

Hellner and Norrman[39] have studied banding in 52100 steel as well as in two tool steels. The banding was studied in steels that had been given an annealing treatment or a quenched and tempering treatment. In the two tool steels, the banding in their micrographs is dominated by primary carbides. However, in the 52100 steel, the banding is due mainly to secondary carbides in wrought samples produced from the top-center of their ingots. They present EPMA data showing that the bands correlate with variations in the alloying elements in these steels. They conclude that the carbide banding is caused by carbon segregation in the solid state, with the carbon diffusing to the bands rich in carbide formers. If this were true, then the carbide banding should also display the characteristic numbered 1 above for hypoeutectoid steels; *i.e.*, the banding should appear after a single cooldown from the austenite region. A series of experiments was carried out on the 52100 steel of Table 1 to examine the nature of carbide banding in this steel.

The as-received 52100 steel was in the spheroidized condition and displayed dark/light bands when etched in picral. The bands were produced by a variation in carbide size and density, and this type of banding will be termed "carbide density banding." Initial experiments were done to see if a banding could be produced in this hypereutectoid steel by a single austenitization and cool. Samples were austenitized at 1100 °C/30 min, and quenching experiments showed this treatment was adequate to dissolve all the carbides. Samples furnace cooled (≈400 °C/h) from this temperature displayed a fine pearlite matrix with thin layers of carbides (<1 μm thick) in the prior austenite grain boundaries and no evidence of banding. The IRs could be located metallographically from the sulfide stringer locations, and there was no change in carbide size at these locations. Hence, it appears that the banding in this hypereutectoid steel differs from that found in hypoeutectoid steels. Whereas a single austenitization/slow cool produces f/p banding in the latter case, it does not produce carbide/p banding in the hypereutectoid 52100 steel.

Additional experiments were carried out to investigate the mechanism of the carbide density banding in the as-received spheroidized steel. This spheroidized condition is generally achieved with a spheroidizing anneal treatment that often consists[59] of austenitization at around 795 °C followed by a very slow cool (≈6 °C/h) from 750 to 675 °C. Samples were first normalized from 1100 °C to remove the as-received banded structure. They were then austenitized at either 900 °C/30 min or at 795 °C/30 min and cooled by either furnace cooling (≈400 °C/h) or at slow programmed cooling rates of around 10 °C/h. Results differed dramatically with the two austenitizing treatments, but no significant difference was observed between the two cooling rates.

Austenitization at 795 °C. Slow cooling from the 795 °C temperature produced a banded microstructure similar to that of the as-received material. Figure 5 presents high magnification micrographs from within neighboring bands showing typical differences in carbide densities that produce the carbide density banding. Samples cooled at the faster furnace cooling rates of ≈400 °C/h displayed very similar structures with carbide diameters that were only very slightly smaller. In both cases, the high density bands corresponded to the IR locations as they were collinear with the sulfide stringers.

To investigate the nature of the carbide formation mechanism, interrupted quench experiments were done in which, following the 795 °C/30 min austenitization, the samples were quenched in water 10 to 20 s after the eutectoid arrest temperature was detected. This technique produced microstructures consisting of the eutectoid transformation product in a martensite matrix, as illustrated in Fig. 6(a). The small black features of Fig. 6(a) are eutectoid transformation products, and the particular region labeled "T" on Fig. 6(a) is shown at high magnification in Fig. 7, where the labels "M" are positioned on top of the martensite phase produced from austenite by the quench. As has been recently discussed,[60] when austenite containing fine carbides undergoes the eutectoid transformation, the reaction may occur by either the famous pearlite transformation or the divorced eutectoid transformation (DET). In the DET reaction, the pre-existing carbides of the matrix simply grow in diameter by around 30% as the transformation front (shown at several points by arrows located at the edge of the martensite regions on Fig. 7) moves past them and converts the matrix phase from austenite to ferrite. The larger transformation products of Fig. 6(a) lie along bands, thus indicating that the DET reaction nucleates first along bands, apparently due to the microsegregation.

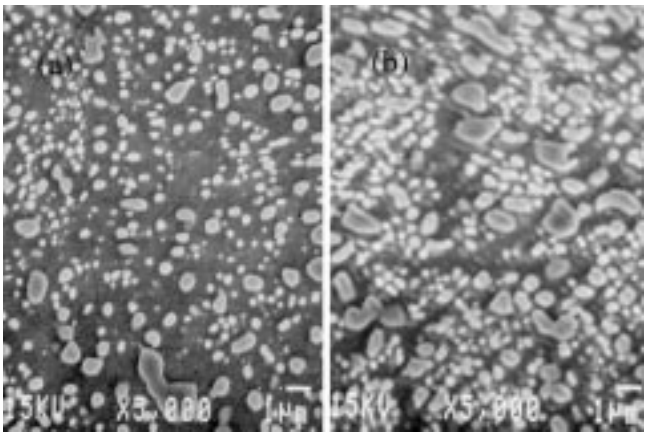

Fig. 5 Microstructure of slow cooled sample, 9 °C/h. **(a)** Low density band. **(b)** High density band. Picral etch

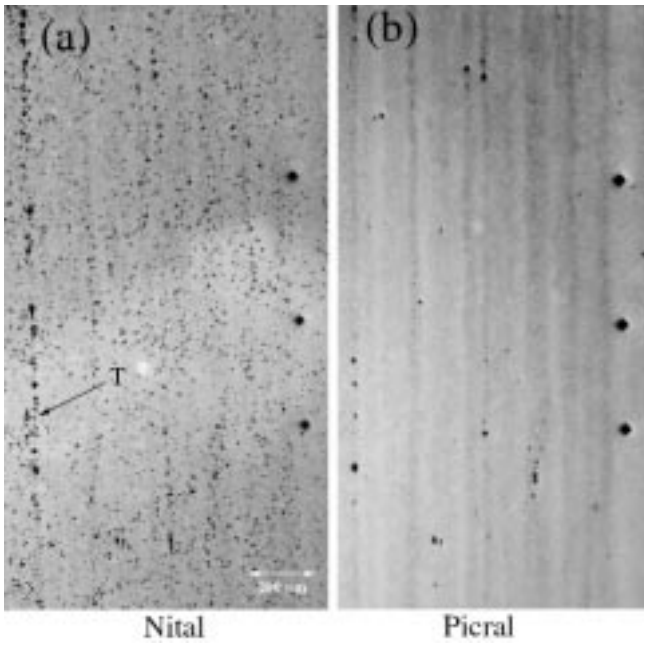

Fig. 6 Interrupted quench sample etched in **(a)** nital and **(b)** picral. Three vertical fiducial microhardness marks on the right. Optical micrographs

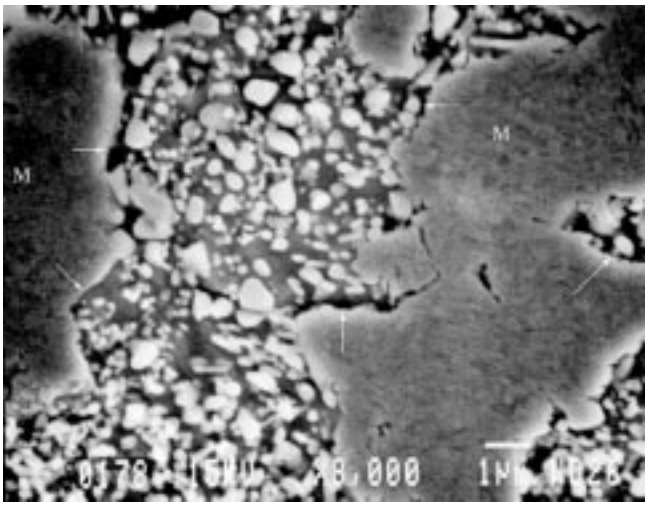

Fig. 7 An enlarged SEM micrograph of region T of Fig. 6**(a)**. Labels M lie over the martensite banding. **(b)** SEM enlargement. Picral etch

Whereas nital etches ferrite much faster than martensite in these samples, as evident in Fig. 7, picral was found to etch the martensite phase and the ferrite phase at similar rates. Hence, the carbides of the martensite matrix and of the ferrite matrix are put into relief by roughly the same amount. As seen in Fig. 6(b), one does not see the DET product phase with a picral etch, except for the largest patches, but a banding is apparent. High magnification scanning electron microscope (SEM) examination shows that the dark/light regions of Fig. 6(b) correspond to differences in carbide density, similar to that shown in Fig. 5. Hence, these results show that the carbide density bands are produced in the austenitization step when the carbides of the original pearlite structure transform to spherical carbide arrays in the austenite matrix. Although the DET appears to nucleate initially along bands, it is unlikely that this process contributes significantly to the final carbide density band morphology, because the density bands are already present in the pre-existing carbides of the austenite prior to the occurrence of the DET.

An experiment was done in which the 52100 steel was water quenched to martensite from 1100 °C and then austenitized at 795 °C and furnace cooled. It displayed the same type of carbide density banding as found with the normalized pearlitic samples. Hence, the formation of carbide density bands upon austenitization occurs whether one starts with a martensitic or a pearlitic structure.

Austenitization at 900 °C. The samples austenitized at 900 °C and furnace cooled displayed prominent banding, as illustrated in Fig. 8(a). The structure consists of alternating bands of (a) pearlite and (b) spheroidized carbides in a ferrite matrix (Fig. 8b). Apparently, upon cooling, the pearlite reaction occurs in one set of bands and the DET reaction in the other set. This result is consistent with formation of carbide density bands discussed above. After initial formation of the carbide density bands at the A_{c1} temperature (found to be around 770 °C) or just above it, one expects the volume fraction carbides to decrease as the temperature continues to rise. Experiments have shown[60] that there is a competition between the pearlite and the DET reactions and, if the pre-existing carbides in the austenite become too large, the pearlite reaction dominates. A likely explanation of the banded structure of Fig. 8 is that at 900 °C the carbides in the initially formed low density carbide bands have dissolved sufficiently to allow the pearlite reaction to dominate, but they remain large enough in the high density bands to allow the DET reaction to dominate. The final ferrite + carbide bands do lie in the initially formed high density carbide bands, as both are collinear with the sulfides.

An alternate form of banding has previously been reported in 52100 steel.[61] Samples were isothermally transformed after austenitization at temperatures high enough to dissolve all carbides. Samples quenched after partial transformation in the pearlite range found no banding of the pearlite formed, but transformation in the bainite range found strong banding of the bainite microconstituent. Hence, with a one cycle heat treatment in the hypereutectoid 52100 steel, it is possible to produce banded structures of (a) bainite/martensite, (b) density banded (carbide + ferrite)/(carbide + ferrite), and (c) pearlite/(carbide + ferrite). However, it does not appear to be possible to produce banded structures of pearlite/(grain boundary carbide) or pearlite/martensite. In both the (b) and (c) structures studied here, the microsegregation must alter the kinetics of the initial formation of the carbides, but the mechanism has not been studied. The high density carbide bands are found to be located where one finds the sulfide inclusions, which means they are occurring in the IRs, which is also where the microsegregated Cr, S, Si, and other elements are located. It may be that more than one mechanism is involved as the high density bands form preferentially on heatup of either a martensite/retained austenite structure or a fine pearlite structure. In the former case, the initial carbides probably nucleate on heatup from the martensite phase, while in the latter case, they probably form from a spheroidization of the

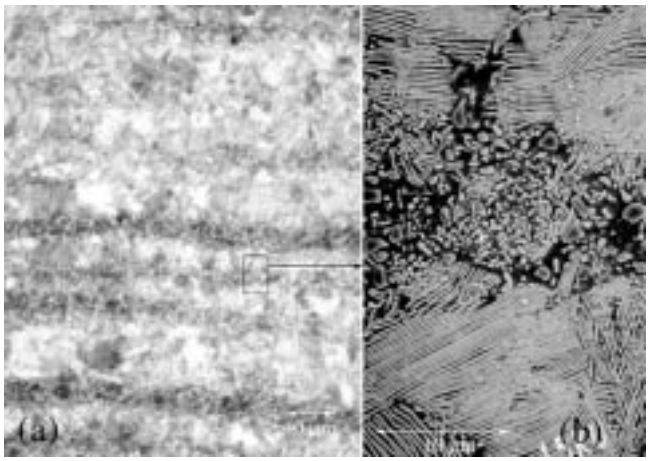

Fig. 8 Austentized at 900 °C/30 min and furnace cooled. **(a)** Optical micrograph showing banding. **(b)** SEM enlargement. Picral etch

carbide component of pearlite as the A_{c1} temperature is exceeded. The pearlite spacing of the normalized starting steel was found to be around 75 nm, which means the carbide lamellae were only around 8 nm thick. Such thin lamellae should quickly spheroidize as the A_{c1} is exceeded. Perhaps the presence of the microsegregated Cr slows the spheroidization rate of the fine carbide lamellae locally and leads to denser carbide bands along the bands of high Cr composition.

6.2 Carbide Banding with Cyclic Heat Treatments

The famous Damascus steel swords of antiquity possess an attractive surface pattern, which is often termed a damascene pattern. Figure 9 presents a seventieth/eighteenth century sword illustrating the damascene pattern. The pattern is produced by bands of carbide particles that are aligned into the plane of the sword blade, as is demonstrated in the sectioned view of the blade shown in Fig. 10. Longitudinal and transverse sections of the blade appear virtually the same, thereby showing that the bands possess a planar geometry as opposed to a lath geometry. The bands are formed by tightly clustered arrays of carbide particles generally having diameters of 5 to 10 μm. Damascus steel swords are relatively pure hypereutectoid plain C steels, as illustrated by the composition of the steel of Fig. 9 given in Table 1. Recent research[57,58] has developed techniques that reproduce both the damascene surface pattern and the internal bands of carbide particles in hypereutectoid steels; and it has been concluded that the microstructure of these swords results from a type of carbide banding requiring cyclic heat treatments for their production. The matrix of the microstructure is controlled by the final thermal cycle. With rapid air cooling, one obtains the (carbide + pearlite)/pearlite banding of Fig. 10. With a furnace cool, the structure becomes (carbide + ferrite)/pearlite as the DET reaction occurs only in the carbide bands. With a quench, the structure becomes (carbide + martensite-retained austenite)/martensite-retained austenite.

The banded structure in the reconstructed Damascus blades is produced as follows. A small, roughly 2.5 kg (5 lb.), ingot of Fe-C-X alloy is prepared with a primary dendrite spacing of 500 to 600 μm, a C level of around 1.5 wt.% C, and the X element identity and composition restricted, as discussed below. The ingot is now forged to a blade shape. It is necessary to carry out the final 10 to 20 forging cycles at temperatures of approximately 100 °C below the A_{cm} temperature of the ingot. Longitudinal sections of the final blades appear virtually identical to Fig. 10, having bands of closely clustered carbide particles in a pearlitic matrix.

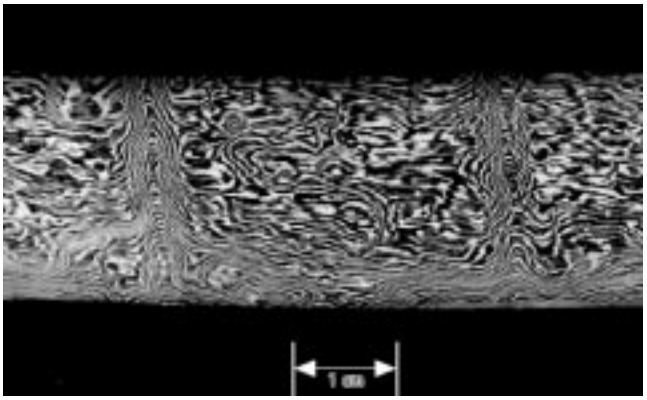

Fig. 9 Damascus sword from Moser collection. Sword 9 of Zschokke.[67] Donated by Ernst Klaey, Bern Museum (Bern, Switzerland)

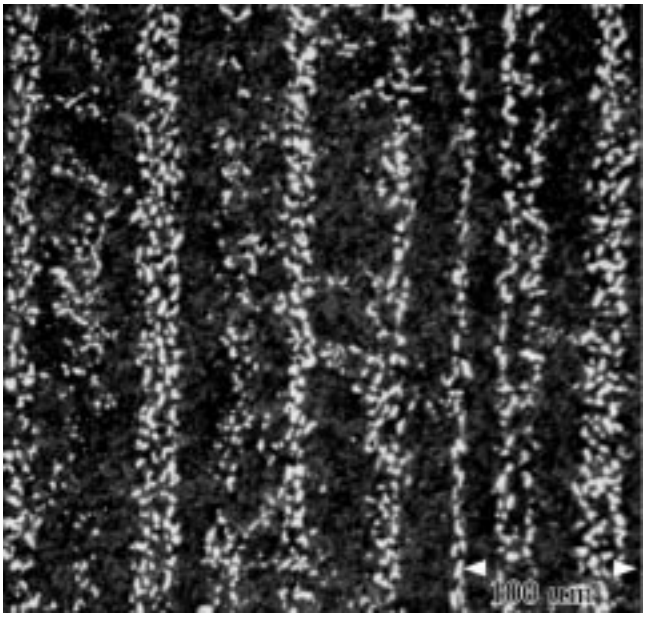

Fig. 10 Longitudinal section of blade of Fig. 9

The formation of the banded structure requires two main restrictions on the process. First, it is necessary to use sufficiently large reductions in the initial stages of the forging to close the IR microporosity that occurs in the hypereutectoid ingots upon solidification. If this is not done, graphite will nucleate in IR micropores[62] and one ends up with bands of graphite stringers rather than with bands of carbide particles. Second, it is necessary to include certain types and composition levels of the X element in the ingot. If the X elements are not included, the carbide particles will not cluster into the bands, but will appear either ran-

domly or in nonbanded arrays. Different levels of band formation and alignment have been found to occur and depend upon the type and amount of the added X element.[63] Strong banding is found with the addition of the carbide forming elements V or Mo at compositions of less than only 0.03%. Weak banding has been found with the addition of either the carbide forming elements, Nb, Cr, and Mn, or S or P at levels of 0.03 to 0.05 %. Steels having these levels of X elements and C levels of 1.1 to 1.8% C will be referred to as Damascus composition steels. The historical blade of Fig. 9 contains 0.005% V, in addition to the elements listed in Table 1.

Whereas the formation of the banding discussed previously occurs on a single cooldown from the austenitizing temperature, the carbide banding of Damascus composition steels requires several repetitive thermal cycles between the austenitizing temperature and room temperature. If a banded Damascus steel is fully austenitized and quenched in water followed by reaustenitization at ≈100 °C below its A_{cm} temperature and air or furnace cooled, one finds no evidence of a banded structure, as the carbides are fairly randomly arrayed. By comparison, the same treatment with the 52100 steel produces strongly banded structures, as illustrated in Fig. 8. However, if the Damascus steel is now thermally cycled between room temperature and ≈100 °C below its A_{cm}, one begins to see faint evidence of banded carbide arrays after two to four cycles, and after around six cycles, the banded arrays become dominant; they appear similar to Fig. 10, except that the carbide particles have smaller diameters.[64] Hence, it is found that the bands of clustered carbide particles in Damascus composition steels require the use of thermal cycling for their formation. This same conclusion is found by examination of the development of microstructure during the forging of ingots to blades. The banded microstructure is observed to form gradually as the number of forging cycles increases.[57]

The following is a review of the evidence showing that microsegregation of the X element plays a key role in the formation of the carbide bands in Damascus composition steels.

- Small pieces of an as-solidified ingot were austenitized and then thermally cycled between room temperature and ≈100 °C below the A_{cm} temperature. If the X element was included in the ingot, a microstructure of clustered arrays of carbide particles lying in the IRs of the ingot was observed. The arrays were identified as lying in the IRs because they appeared with the characteristic outline of dendrite arrays. In addition, the microporosity and the FeS particles were also found within the arrays. If the X element was not included, the cycled ingot pieces displayed carbides only in random arrays. The experiments showed that the X element addition causes the carbides to form on thermal cycling as clustered particles in the IRs.[58]
- Two pieces of a hypoeutectoid blade with the banded structure similar to Fig. 10 were austenitized and quenched to destroy the banded microstructure. One piece was then thermally cycled six times between room temperature and ≈100 °C below its A_{cm} temperature. The banded microstructure returned. The other piece was heated to 1250 °C and held for 18 h. After this treatment, it was given the same six cycle thermal treatment as the first piece, but the banded microstructure did not form; the carbide particles remained in random arrays. Calculations show that an 18 h heat treatment at 1250 °C is adequate to homogenize microsegregation of typical substitutional alloy elements in austenite. Hence, the results present strong evidence that microsegregation of the X element causes the banding to occur.[65]
- An electron microprobe study[63] was carried out on Fe-C-X alloys with X elements such as V present at the low levels of 0.035%. The DRs were located by finding the FeS particles, which were present in these ingots with S levels of 0.003 to 0.008%. A significant microsegregation of V and similar elements was found in the DRs. For example, V carbides were found in the IRs and V levels of 0.6 to 1.4% were found in the M_3C carbides located there, even though the overall V level of the ingots was only 0.035%. The studies show that a strong microsegregation of the X elements occurs during ingot formation. In addition, a study of several ancient Damascus blades [66] similar to Fig. 9 consistently found the presence of carbide forming X elements, particularly V, at levels of 0.004% and above, showing that low levels of carbide forming elements were present in these Damascus steels.

The above data present strong evidence that the carbide banding of Damascus composition alloys is produced by microsegregation of the X element in the original ingots. Furthermore, it shows that the bands of clustered carbide particles form by some mechanism that requires thermal cycling between room temperature and a temperature just below the A_{cm} temperature. The mechanism of formation of the carbides clustered selectively along the IRs during the cyclic heating of the forging process is not resolved. It seems likely, however, that it involves a selective coarsening process, whereby carbide particles lying on the IRs slowly become larger than their neighbors lying on dendrite regions and crowd them out. A model for such a selective coarsening process has been presented.[58] During the heatup part of each thermal cycle, the smaller carbide particles will dissolve and only the larger particles will remain at the forging temperature, which lies just below the A_{cm} temperature. The model requires the segregated impurity atoms lying in the IRs to selectively reduce the mobility of the carbide/austenite interfaces in those regions. Larger particles would then occur in the IRs at the forging temperature. They would maintain their dominance on cooldown because one would not expect the small particles that had dissolved to renucleate on cooldown in the presence of the nearby carbide particles. These nearby particles would provide sites for carbide growth on cooling prior to adequate local supercooling sufficient to nucleate new particles. The EPMA study[63] provides some indirect evidence to support this model, as the increased composition levels of carbide forming elements such as V in the IR carbides means that they are partitioning to the IR carbides, an effect that would be expected to slow the carbide growth rates selectively in the IRs.

7. Summary and Conclusions

A review of the very large literature on banding in hypoeutectoid steels has identified several characteristics of this phenomenon and pointed out a few areas where further research would be helpful. The literature on banding in hypereutectoid

steels was found to be quite sparse, and banding experiments are presented on 52100 steel. They show that the banding by secondary carbide formation is similar to banding in hypoeutectoid steels in that it occurs on a single-thermal cycle, but the mechanism is quite different, often involving the DET. A distinct type of carbide banding can be made to form in relatively pure hypereutectoid steels, which differs from the banding found in commercial hypereutectoid steels because of the requirement of thermal cycling. This type of banding occurs in Damascus composition steels and requires the addition of low levels of carbide forming elements, such as V or Mo, Its mechanism is thought to involve a preferred coarsening of the carbides in IR bands during the thermal cycling.

Acknowledgments

This work was sponsored jointly by funds from Iowa State University and the United States Department of Energy, Office of Basic Energy Sciences, through the Ames Laboratory, Iowa State University, Contract No. W-7405-ENG-82.

References

1. J.E. Stead: *J. Soc. Chem. Ind.,* 1913, vol. 33, pp. 173–84.
2. J.E. Stead: *J. Iron Steel Inst.,* 1915, vol. 91, pp. 140–81.
3. P. Oberhoffer: *Stahl Eisen,* 1913, vol. 33, pp. 1569–74.
4. P. Oberhoffer: *Z. Anorg. Chem.,* 1913, vol. 81, pp. 156–69.
5. P. Oberhoffer and H. Meyer: *Stahl Eisen,* 1914, vol. 34, 1241–45.
6. J.E. Stead: *J. Iron Steel Inst.,* 1918, vol. 103 pp. 287–92.
7. H.C.H. Carpenter and J.M. Robertson: *J. Iron Steel Inst.,* 1931, vol. 118 pp. 345–79.
8. H.M. Howe: *The Metallography of Steel and Cast Iron,* McGraw-Hill, New York, NY, 1916, pp. 556–65
9. A.E. Cameron and G.B. Waterhouse: *J. Iron Steel Inst.,* 1926, vol. 113, p 355–74.
10. J.H. Whitely: *J. Iron Steel Inst.,* 1926, vol. 113, p 213–18.
11. P.G. Bastien; *J. Iron Steel Inst.,* 1957, vol. 174, pp. 281–90.
12. L.E. Samuals: *Optical Microscopy of Carbon Steels,* ASM, Metals Park, OH, 1980, pp. 127–35.
13. J.S. Kirkaldy, J. von Destinon-Forstmann, and R. J. Brigham: *Can. Met. Q.,* 1962, vol. 1, p 59–81.
14. T.W. Clyne and W. Kurz: *Metall. Trans. A,* 1981, vol. 12A, pp. 965–71.
15. J.S. Kirkaldy and G.R. Purdy: *Can. J. Phys.,* 1962, vol. 40, 208–17.
16. L.C. Brown and J.S. Kirkaldy: *Trans. TMS-AIME,* 1964, vol. 230, p 223–26.
17. H.L. Geiger: *Met. Progr.,* 1933, vol. 23 (2), pp. 37–40.
18. R. Grossterlinden, R. Kawalla, U. Lotter, and H. Pircher: *Steel Res.,* 1992, vol. 63, p 331–36.
19. J.H. Whiteley: *J. Iron Steel Inst.,* 1935, vol. 131, No. I, p 181–211.
20. J.D. Lavender and F.W. Jones: *J. Iron Steel Inst.,* 1949, vol. 163, p 14–17.
21. E.T. Turkdogan and R.A. Grange: *J. Iron Steel Inst.,* 1970, vol. 208, pp. 482–94.
22. A. Kohn and J. Doumerc: *Rev. Met.,* 1955, vol. 52 (3), pp. 249–57.
23. J. Philibert and H. Bizouard: *Mem. Sci. Rev. Met.,* 1959, vol. 56, p 187–97.
24. A. Pokorny and J. Pokorny: *De Ferri Metallographia,* vol. 3, *Solidification and Deformation of Steels,* Berger-Lerrault, Paris, 1967, pp. 95–103.
25. L. Hellner and T.O. Norrman: *Jernkont. Ann.,* 1968, vol. 152, p 269–86.
26. S.W. Thompson and P.R. Howell: *Mater. Sci. Technol.,* 1992, vol. 8, p 777–84.
27. J. Delorme, P. Martin, C. Rocques, and P. Bastien: *Mem. Sci. Rev. Met.,* 1961, Vol. 58, p 424–34.
28. R.M. Fisher, G.R. Speich, L.J. Cuddy, and H. Hu: *Physical Chemistry in Metallurgy: Proceedings of the Darken Conference,* R.M. Fisher, R.A. Oriani, and E.T. Turkdogan, eds., United States Steel, Monroeville, PA, 1976, pp. 466–73.
29. F.A. Heiser and R.W. Hertzberg: *J. Iron Steel Inst.,* 1971, vol. 209, pp. 975–80.
30. C.F. Jatcak. D.J. Girardi, and E.S. Rowland: *Trans. ASM,* 1956, vol. 48, p 279–305.
31. G. Mukherjee: *Tool Alloy Steel,* 1977 vol. 11 (2), pp. 55–58.
32. T.B. Smith: *J. Iron Steel Inst.,* 1963, vol. 200, p 602–09.
33. R.A. Grange: *Metall. Trans.,* 1971, vol. 2, p 417–26.
34. M.A. Portevin: *Rev. Metall.,* 1913, vol. 10, p 689–91.
35. F.C. Thompson and R. Willows: *J. Iron Steel Inst.,* 1931, vol. 124, p 151–76.
36. H.C.H. Carpenter and J.M. Robertson: *J. Iron Steel Inst.,* 1933, vol. 127, p 259–84.
37. J.H. Whiteley: *Metallurgist,* 1926, vol. 2, pp. 125–26.
38. W. Peter and H. Finkler: *Harterer Techn. Mitt.,* 1961, vol. 16 (3), pp. 51–60.
39. L. Hellner and T.O. Norrman: *Jernkont. Ann.,* 1968, vol. 152, p 269–86.
40. J.A. Eckert, P.R. Howell, and S.W. Thompson: *J. Mater. Sci.,* 1993, vol. 28, p 4412–20.
41. C.B. Voldrich: *Suppl. J. Am. Welding Soc.,* 1947, vol. 26, p 153s–169s.
42. E.R. Johnson and W.J. Buechling: *Trans. ASM,* 1934, vol. 22, p 249–65.
43. H. Schwartzbart: *Trans. ASM,* 1952 vol. 44, p 845–52.
44. W.A. Spitzig: *Metall. Trans., A* 1983 vol. 14A, p 271–83.
45. U. Wyss: *Arch. Eisenhuttenwes,* 1956, vol. 22, pp. 258–60.
46. J.H. Whiteley: *J. Iron Steel Inst.,* 1931, vol. 123 (I), p 385–87.
47. J.B. Sychterz, M.P. Marino, and P.R. Howell: *Can. Inst. Min. Met. Petr.,* 1995, pp. 135–46.
48. H.G. Kim and P.R. Howell: in *Microstructural Banding in Isothermally Transformed Hypoeutectoid Steels, Solid/Solid Phase Transformations,* W.C. Johnson, J.M. Howe, D.E. Laughlin, and W.A. Soffa, eds., TMS, Warrendale, PA, 1994, pp. 183–88.
49. T. Berg: *Trans. Am. Soc. Steel Treatment,* 1934, vol. 22, 265–66.
50. A.S. Bor: *Iron Steel Inst. Jpn. Int.,* 1991, vol. 31, p 1445–46.
51. H. Brearley: *Proc. Sheffield Soc. Eng. Met.,* 1909, vol. 2, p. 56.
52. M. Ziegler: *Rev. Met.,* 1911, vol. 8, p 655–72.
53. E.G. Mahin and E.H. Hartwig: *J. Ind. Eng. Chem.,* 1920, vol. 12, pp. 1090–95.
54. J.S. Kirkaldy, R.J. Brigham, H.A. Domian, and R.G. Ward: *Can. Met. Q.,* 1963, vol. 2, p 233–41.
55. R. Kiessling: *Non-Metallic Inclusions in Steel,* Part V, The Metals Society, London, 1978, pp. 173–77.
56. H. Jacobi and K. Schwerdtfeger: *Metall. Trans. A* 1976, vol. 7A, pp. 811–20.
57. J.D. Verhoeven and A.H. Pendray: *Mater. Characterization,* 1992, vol. 29, p 195–212.
58. J.D. Verhoeven, A.H. Pendray, and E.D. Gibson: *Mater. Characterization,* 1996, vol. 37, p 9–22.
59. *Heat Treater's Guide,* 2nd ed., ASM INTERNATIONAL, Materials Park, OH, 1995, p. 429.
60. J.D. Verhoeven and E.D. Gibson: *Metall. Mater. Trans.,* 1998, vol. 29A, pp. 1181–89.
61. C.A. Stickels: *Metall. Trans.,* 1974, vol. 5, pp. 865–74.
62. P.M. Berge, J.D. Verhoeven, D.T. Peterson, and A.H. Pendray: *Iron Steelmaker,* 1995, vol. 22 (3), pp. 67–72.
63. J.D. Verhoeven, F. Laabs, A.H. Pendray, and W.E. Dauksch: *ISS Trans.,* 1998, vol. 25, p 65–74.
64. J.D. Verhoeven and A.H. Pendray: *Mater. Characterization,* 1993, vol. 30, p 175–86.
65. J.D. Verhoeven, A.H. Pendray, and P.M. Berge: *Mater. Characterization,* 1993, vol. 30, p 187–200.
66. J.D. Verhoeven, A.H. Pendray, and W.E. Dauksch: *J. Met.,* 1998, vol. 50, No. 9, p 58–64.
67. B. Zschokke: *Rev. Met.,* 1924, vol. 21, p 635–39.